01

Self-broadening of absorption and isotropic Raman scattering lines of acetylene: classical impact theory calculations in a wide temperature range

© S.V. Ivanov

SRC „Kurchatov Institute“, FSRC „Crystallography and Photonics“,
Moscow, Russia

e-mail: serg.ivanov.home@mail.ru

Received June 02, 2025
Revised October 11, 2025
Accepted October 13, 2025

A method of self consistent classical trajectory simulation of $C_2H_2-C_2H_2$ collisions has been developed. The explicitly derived equations of motion are used to calculate the vibration-rotational collisional widths of absorption lines and isotropic Raman scattering lines of acetylene within the framework of classical impact theory. Dynamic calculations were performed using the simplest atom−atomic + quadrupole−quadrupole intermolecular $C_2H_2-C_2H_2$ interaction potential. The J-dependences of the self-broadening coefficients of the $^{12}C_2H_2$ lines in the temperature range from 150 to 700 K, as well as the exponents of temperature dependence of broadening, are calculated. A comparison is made with the available experimental data. The contribution of collisions of different types (elastic, inelastic, collision complexes) to the self-broadening of lines, as well as the role of the value of the C_2H_2 electric quadrupole moment, is analyzed

Keywords: acetylene, vibration-rotational lines, collisional broadening, classical impact theory, classical trajectory method, intermolecular interactions, collision complexes.

DOI: 10.61011/EOS.2025.10.62565.8238-25

1. Introduction

Acetylene is a linear symmetric molecule (chemical formula C_2H_2, structural formula H−C=C−H, point group $D_{\infty h}$). It has five normal vibrational modes: $\nu_1 = 3373.7\,\text{cm}^{-1}$, $\nu_2 = 1973.8\,\text{cm}^{-1}$, $\nu_3 = 3287\,\text{cm}^{-1}$, $\nu_4 = 611.8\,\text{cm}^{-1}$, $\nu_5 = 729.1\,\text{cm}^{-1}$ [1]. The spectrum of C_2H_2 in the 14 μm region (band ν_5) has been observed in the atmospheres of Jupiter, Saturn, and Titan [2,3]. Acetylene has diverse practical applications. Its primary feature is the ability to provide and sustain a flame temperature of up to 3150 °C. Traditionally, C_2H_2 in cylinders is used for welding and cutting metal products (in combination with oxygen). C_2H_2 is also employed in autonomous lighting devices (source of bright white light in lighthouse lamps, ship lighting, and so on) Acetylene is used in medicine (component for anesthesia, smoking biomarker in exhaled air [4]), industry (production of organic synthesis products: acids, rubber, polymers, solvents, and so forth). During combustion, acetylene forms through the oxidation of hydrocarbon fuel and acts as a precursor to soot formation, which has carcinogenic effects [5]. Quantitative measurements of C_2H_2 content in combustion processes are crucial for assessing the environmental impact of various fuel types [6].

In the Earth's atmosphere, C_2H_2 is one of the minor gaseous components and is formed primarily through the photodissociation of methane [7] and the combustion of fossil fuels. In unpolluted air, its concentration is very low (< 0.5 ppbV). However, due to the rapid growth of automobile transport, a noticeable increase in the atmospheric concentration of C_2H_2 can be expected in the future [7]. As a result, in the long term, acetylene may become another greenhouse gas.

Given this context, studying the spectra of C_2H_2 in various mixtures over a wide temperature range holds significant scientific and practical value. Numerous experimental and theoretical studies of the infrared (IR) spectra of acetylene have focused on the broadening of vibrational-rotational lines in various fundamental and combination bands in mixtures with N_2, O_2, H_2 and noble gases [8–22]. Works [15,16] provide comprehensive review information on the broadening of C_2H_2 lines by nitrogen, directly relevant to the Earth's atmosphere.

In recent decades, interest in the self-broadening of acetylene lines has grown substantially. Self-broadening coefficients for C_2H_2 have been investigated experimentally and/or theoretically (primarily within the semiclassical Robert-Bonamy method) in various absorption bands: ν_5 [23–25], $\nu_4+\nu_5$ [26–28], $2\nu_4+\nu_5$ and $3\nu_5$ [26], $\nu_1+\nu_5$ [9,29], $\nu_1+3\nu_3$ [30–33], $\nu_1+\nu_3$ [34–43], $5\nu_3$ [44], $\nu_1+\nu_2+\nu_4+\nu_5$ [45,46], $\nu_1+\nu_3+\nu_4-\nu_4$ [47]. Due to experimental challenges, most measurements were conducted over relatively narrow temperature ranges (mostly at room temperature and below) and limited ranges of the rotational quantum number J.

In this paper, the classical impact theory of Gordon is used to calculate the self-broadening of vibrational-rotational absorption lines and isotropic Raman scattering lines of

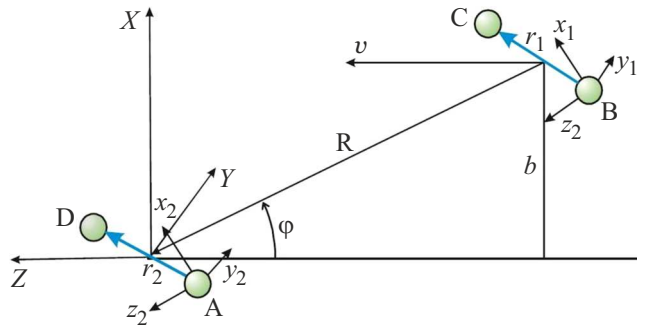

Figure 1. Schematic of the collision between rotator „1“ (BC) and rotator „2“ (AD) [48]. (X, Y, Z) — laboratory coordinate system; (x_1, y_1, z_1) and (x_2, y_2, z_2) — molecule-fixed coordinate systems.

acetylene. J-dependencies of the self-broadening coefficients for C_2H_2 lines ($J \leq 40$) were computed over a temperature range from 150 to 700 K. Comparisons with selected experimental data were performed. The contributions of various collision types to broadening (elastic, inelastic, collision complexes) were analyzed, along with the role of the electric quadrupole moment of C_2H_2.

The article is organized as follows. Section 2 presents the basic equations of collision dynamics and the classical impact theory for isolated spectral lines. Section 3 describes the intermolecular potential energy surface for C_2H_2–C_2H_2 used in the calculations. Details of the trajectory calculations are given in Section 4. Section 5 is devoted to the results and their discussion. Conclusions are formulated in Section 6.

2. Basic Equations

2.1. Collision Dynamics

Consider a system of interacting quasi-diatomic linear molecules (rotators) BC („1“, active molecule) and AD („2“, buffer molecule) (Fig. 1). The collision geometry can be described using the following variables: the intermolecular distance vector $\mathbf{R}(t)$ directed from the center of mass of rotator BC to the center of mass of rotator AD, and two sets of molecule-fixed coordinates (x_1, y_1, z_1) and (x_2, y_2, z_2), which define the orientations of the molecular axes $\mathbf{r}_1$ and $\mathbf{r}_2$ in their respective coordinate systems. The centers of the molecule-fixed coordinates are located at one of the terminal atoms of the corresponding molecule (B and A), with the axes z_1, z_2 of the coordinate systems always directed along the vector $\mathbf{R}$. The center of mass of rotator AD is at rest, and rotator BC has an initial relative velocity v, the vector of which is parallel to the Z axis of the laboratory coordinate system.

The exact 3D classical Hamiltonian for the system of rigid rotators BC–AD has the form

$$H = T + V(\mathbf{R}, \mathbf{r}_1, \mathbf{r}_2), \tag{1}$$

$$T = \frac{p_R^2}{2\mu_{\mathrm{AD,BC}}} + \frac{L^2}{2\mu_{\mathrm{AD,BC}}R^2} + \frac{p_{x1}^2 + p_{y1}^2 + p_{z1}^2}{2\mu_{\mathrm{BC}}} + \frac{p_{x2}^2 + p_{y2}^2 + p_{z2}^2}{2\mu_{\mathrm{AD}}},$$

$$L^2 = \mu_{\mathrm{AD,BC}}R^4(\dot{\theta}^2 \sin^2\varphi + \dot{\varphi}^2).$$

Here, T — kinetic energy of the AD–BC system, L and $\mu_{\mathrm{AD,BC}}$ — orbital angular momentum and reduced mass of the colliding pair, μ_{BC} and μ_{AD} — reduced masses of molecules BC and AD. The angle φ — elevation angle (angle between vector $\mathbf{R}$ and the YZ plane of the laboratory coordinate system), θ — rotation angle of the collision plane relative to the initial position (see [48] for details). The intermolecular interaction potential $V(\mathbf{R}, \mathbf{r}_1, \mathbf{r}_2) = V(R, \gamma_1, \gamma_2, \phi)$ is four-dimensional. It is determined by the Jacobi coordinates — the distance between centers of mass R and three orientational angles: γ_1, γ_2 (γ_1 — angle between vectors$\mathbf{R}$ and $\mathbf{r}_1$, γ_2 — between $\mathbf{R}$ and $\mathbf{r}_2$) and the angle ϕ between the planes containing vectors $\mathbf{R}$, $\mathbf{r}_1$ and $\mathbf{R}$, $\mathbf{r}_2$ (the so-called „twist“ angle). Note that for identical molecules,$r_1 = r_2$ and $\mu_{\mathrm{BC}} = \mu_{\mathrm{AD}}$.

The Hamilton equations describing the classical dynamics of the AD–BC system have the standard [49] form:

$$\dot{q}_i = \frac{\partial H}{\partial p_i}, \quad \dot{p}_i = -\frac{\partial H}{\partial q_i}, \quad i = 1, 2, \ldots, i_{\max}, \tag{2}$$

where q_i and p_i — generalized coordinates and conjugate momenta. For the case of two rigid rotators, $i_{\max} = 9$ ($q_1 - q_9 = R, \varphi, \theta, x_1, y_1, z_1, x_2, y_2, z_2$; $p_1 - p_9 = p_R, p_\varphi, p_\theta, p_{x1}, p_{y1}, p_{z1}, p_{x2}, p_{y2}, p_{z2}$), (x_1, y_1, z_1) — coordinates of atom C relative to atom B and (x_2, y_2, z_2) — coordinates of atom D relative to atom A (see [48] for details). Substituting the Hamiltonian (1) into equations (2) yields 17 (since $p_\theta = \mathrm{const}$) exact self-consistent classical equations of motion, the explicit form of which is given in the Appendix at the end of the article. Note that these equations are published in the Russian literature for the first time.

2.2. Basic Formulas of the Classical Impact Theory

In Gordon's classical impact theory, the half-width γ of an isolated vibrational-rotational line of electric dipole absorption is described [50] by the formula

$$\gamma = \frac{n_b}{2\pi c}\left\langle v \cdot [1 - P_{el}\cos\eta\cos^2(\alpha/2)]\right\rangle_{b,v,O,\omega_2}. \tag{3}$$

Equation (3) accounts for contributions from both inelastic and elastic collisions. For Q-lines of isotropic Raman scattering, only the contribution from rotationally inelastic collisions is significant [50,51]:

$$\gamma = \frac{n_b}{2\pi c}\langle v \cdot (1 - P_{el})\rangle_{b,v,O,\omega_2}. \tag{4}$$

In equations (3), (4) n_b — number density of perturbing particles (here — all otherC_2H_2, molecules surrounding the one under consideration), c — speed of light. P_{el} — probability (index) that a given collision is elastic/inelastic. As shown in [48] for the example of N_2, the best agreement with experiment is achieved by computing P_{el} using the box quantization procedure ($P_{el} = 1$ for elastic collisions and $P_{el} = 0$ for inelastic ones). The statistical averaging of $\langle \ldots \rangle$ is performed over the impact parameter b, relative velocity of the pair v, initial orientations O of the unit vectors of the molecular axes $\mathbf{r}_1, \mathbf{r}_2$ of both molecules, and their angular velocities $\boldsymbol{\omega}_1$, $\boldsymbol{\omega}_2$, as well as the modulus ω_2. The angle η characterizes „rotational dephasing", while α — the angle between the initial and final orientations of the vector $\boldsymbol{\omega}_1$ („rotational reorientation"). Values of η and α are computed from the classical dynamics of each specific collision using the modified method described in the Appendix of [52]. Formulas (3) and (4) do not account for vibrational phase shifts (so-called „vibrational dephasing" [51]), as the molecules are treated as rigid. This approximation is quite acceptable in the present case, since measurements of broadening in a number of acetylene bands show weak vibrational dependence [26,28].

3. Intermolecular Interaction Potential $C_2H_2-C_2H_2$

In these classical calculations, a simple potential energy surface (PES) for the intermolecular interaction $C_2H_2-C_2H_2$ of the atom−atom + quadrupole−quadrupole type ($aa + QQ$) from the work of Lambo et al. [24] was employed:

$$V(\mathbf{R},\ \mathbf{r}_1, \mathbf{r}_2) = V_{aa}(\mathbf{R},\ \mathbf{r}_1, \mathbf{r}_2) + V_{QQ}(\mathbf{R},\ \mathbf{r}_1, \mathbf{r}_2). \qquad (5)$$

The atom−atom interaction term has the form

$$V_{aa} = \sum_{i,j}\left(\frac{d_{ij}}{r_{1i,2j}^{12}} - \frac{e_{ij}}{r_{1i,2j}^{6}}\right), \qquad (6)$$

where $r_{1i,2j}$ — distances between atom i of molecule „1" and atom j of the molecule „2", e_{ij} and d_{ij} — parameters for the corresponding atomic pair. The long-range quadrupole−quadrupole interaction term is described in the standard manner [53]:

$$V_{QQ} = \frac{3Q_1Q_2}{4R^5} \cdot f(\gamma_1, \gamma_2, \varphi_1, \varphi_2), \qquad (7)$$

$$f(\gamma_1, \gamma_2, \varphi_1, \varphi_2) =$$

$$= 1 - 5(\cos^2\gamma_1 + \cos^2\gamma_2 + 3\cos^2\gamma_1\cos^2\gamma_2)$$

$$+ 2\left[4\cos\gamma_1\cos\gamma_2 - \sin\gamma_1\sin\gamma_2 \cdot \cos(\varphi_1 - \varphi_1)\right]^2.$$

Here, Q_1, Q_2 — electric quadrupole moments of molecules „1" and „2"; γ_1 and γ_2 — angles between the molecular axes $\mathbf{r}_1$, $\mathbf{r}_2$ and the vector $\mathbf{R}$ (polar angles); φ_1 and φ_2 — corresponding azimuthal angles in the molecule-fixed coordinate systems of molecules„1" (BC) and „2" (AD). Note once again that the axes z_1 and z_2 of the molecule-fixed coordinate systems are always directed along the vector $\mathbf{R}$.

Table. Parameters of the atom-atom potential V_{aa} for the system $C_2H_2-C_2H_2$ [24]

e_{ij} (10^{-11} erg Å^6)	d_{ij} (10^{-8} erg Å^{12})	r_{1i} (Å)
$e_{\text{H–H}} = 0.235$	$d_{\text{H–H}} = 0.117$	$\lvert r_{1\text{H}}\rvert = 1.6614$
$e_{\text{H–C}} = 0.419$	$e_{\text{H–C}} = 0.202$	
$e_{\text{C–C}} = 0.747$	$d_{\text{C–C}} = 0.349$	$\lvert r_{1\text{C}}\rvert = 0.6035$

In the case under consideration for the $C_2H_2-C_2H_2$ system, molecules „1" and „2" are identical and, hence, $Q_1 = Q_2 = Q$. The coefficients e_{ij}, d_{ij} and intramolecular distances $r_{1\text{H}}$, $r_{1\text{C}}$(distances from the center of mass of the H−C=C−H molecule to the H and C atoms, respectively) are given in the table.

As in [24], the electric quadrupole moment of C_2H_2 used in the calculations was $Q = 5.42$ DÅ (5.42 ± 0.41 DÅ according to measurements [54]). The hexadecapole moment of C_2H_2 and higher-order multipole moments were neglected in these calculations.

4. Details of trajectory calculations

Classical 3D trajectory calculations (C3D) were performed using the method described in detail previously for the N_2-N_2 system [48]. Only a correction related to the buffer molecule (also C_2H_2) was introduced: its initial J_2-states (J_2 — rotational quantum number of molecule AD) were selected discretely, accounting for nuclear spin degeneracy $g_I = (-1)^{J_2+1} + 2$. As a result, for *ortho* levels of C_2H_2 (odd J_2) we have $g_I = 3$, while for *para* levels (even J_2) $g_I = 1$. However, this modification did not lead to noticeable differences in the results compared to continuous selection of initial J_2-states without accounting for spin degeneracy.

The initial rotational angular frequency ω_1 of the target BC molecule was determined from the initial rotational quantum number J (Langer correction or „prescription" [55,56]) using the average J value for the optical transition under consideration [50,51]:

$$I\omega_1 = \hbar\left(J_{\text{average}} + \frac{1}{2}\right), \qquad (8)$$

where I —moment of inertia of the rotator, $\hbar$ — Planck's constant. The values of J_{average} for various branches of the vibrational-rotational band are as follows:

$$P - \text{lines},\ \Delta J = -1,\ J_{\text{average}} = \frac{J + (J-1)}{2} = J - 1/2,$$

$$Q - \text{lines},\ \Delta J = 0,\ J_{\text{average}} = \frac{J + J}{2} = J,$$

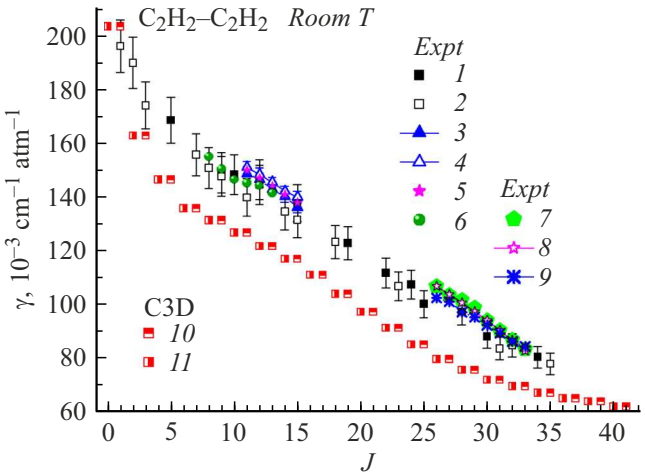

Figure 2. Self-broadening of C_2H_2 absorption lines: comparison of C3D calculations with experiment at room temperature. Experiment: *1* — ν_5 *P*-branch [24] ($T = 298$ K), *2* — ν_5 *R*-branch [24] ($T = 298$ K), *3* — lines in the *P*branch of the $\nu_1 + \nu_3$band [37] Voigt profile, *4* — [37] Rautian profile, *5* — [37] — HITRAN2008 ($T = 296$ K), *6* — [41], lines in the *R*-branch of the $\nu_1 + \nu_3$ band ($T = 295-300$ K), *7* — [28] ($T = 296$ K), *8* — [28] — HITRAN2012, *9* — [28,26]. Present C3D calculations ($T = 298$ K): *10* — *P*-branch, *11* — *R*-branch. PES of type $aa + QQ$, $Q = 5.42$ DÅ.

$$R-\text{lines},\ \Delta J = +1,\ J_{\text{average}} = \frac{J + (J+1)}{2} = J + 1/2. \tag{9}$$

The Langer correction in the form (8),(9) provides better (in terms of agreement with experiment) broadening coefficients for low values J (especially for $J = 0$) than the traditional angular momentum quantization formula [57]. As J increases, the effect of this correction rapidly diminishes.

The Monte Carlo method was used to select the initial orientations of vectors $\mathbf{r}_1$, $\mathbf{r}_2$ and $\boldsymbol{\omega}_1$, $\boldsymbol{\omega}_2$ uniformly distributed in 3D space under the condition of orthogonality$\mathbf{r}_1 \perp \boldsymbol{\omega}_1$, $\mathbf{r}_2 \perp \boldsymbol{\omega}_2$. In all calculations, Maxwellian averaging over the initial relative velocity was applied in the interval $v = (0.01 \div 3)v_p$, where $v_p = (2k_BT/\mu_{AD,BC})^{1/2}$ — most probable relative velocity of the colliding pair (T — temperature, k_B — Boltzmann constant, $\mu_{AD,BC} = 13$ a.m.u. for $^{12}C_2H_2-^{12}C_2H_2$). The maximum impact parameter was set to $b_{max} = 12$ Å. The root-mean-square error of the calculated line half-widths was maintained at less than 1%. Auxiliary calculations at $b_{max} = 10$, 12, 14 Å and $T = 150$ K, as well as at$b_{max} = 12$, 13 Å and $T = 298$ K showed that the impact parameter range $b \le b_{max} = 12$ Å is fully sufficient for modeling the self-broadening of C_2H_2 lines at temperatures of 150–700 K.

In all calculations, an efficient algorithm [56] for sampling the impact parameter b was employed. In this case, the convergence of the Monte Carlo method is approximately twice as fast as with traditional uniform sampling over b^2. The calculations showed that the laws of conservation of energy and angular momentum are satisfied with high accuracy for the vast majority of trajectories.

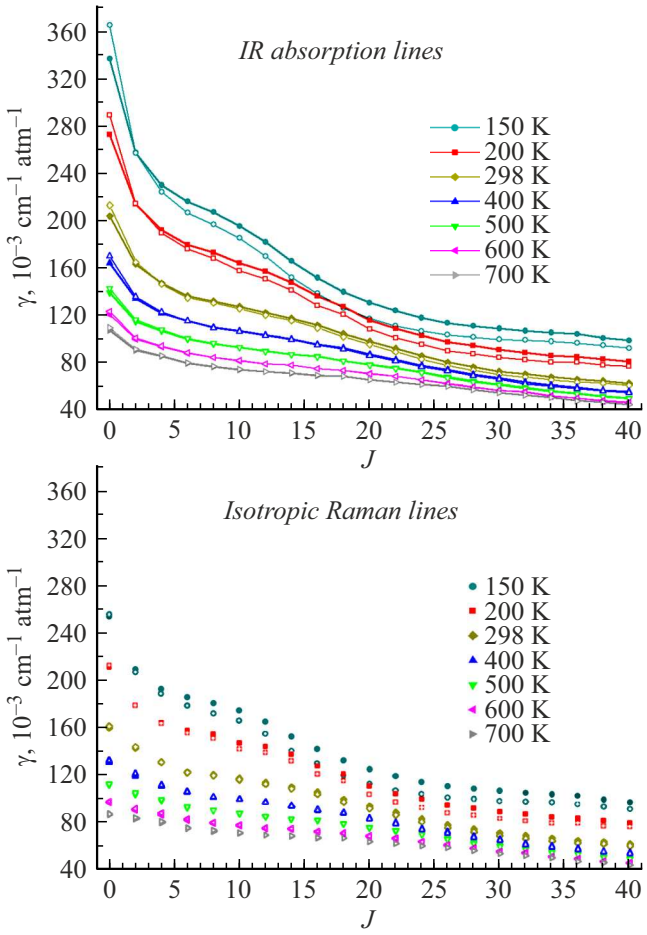

Figure 3. *a* — self-broadening of IR absorption lines in the ν_5 band of C_2H_2; *b* — self-broadening of *Q*-lines of isotropic Raman scattering of C_2H_2. C3D calculations using the $aa + QQ$ PES at various temperatures. Filled symbols — accounting for all collision types, open symbols — without collision complexes. $Q = 5.42$ DÅ.

The Hamilton equations were numerically integrated using the standard procedure from the IMSL library (Gear's implicit BDF method [58]). Calculations were performed with double precision with a typical stability parameter TOL $= 10^{-8}$ and a variable integration step within fixed time grid intervals of $\Delta t = 5$ ps. The trajectories began and ended at $R_{max} = 15$ Å.

5. Results and Discussion

The results of C3D calculations and measurements of self-broadening coefficients for C_2H_2 absorption lines at room temperature are compared in Fig. 2. The basic experimental data correspond to Table 1 of [24]. The main sources of error in measuring broadening coefficients arose from inaccuracies in the baseline position and the presence of weak overlapping transitions, mainly from hot bands $2\nu_5-\nu_5$

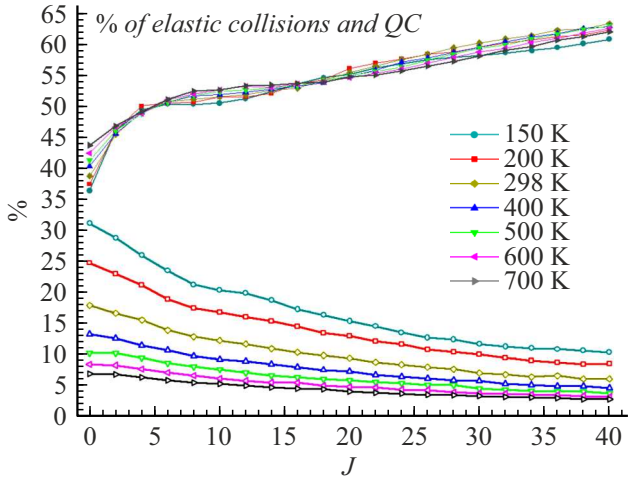

Figure 4. Fractions of elastic collisions (filled symbols) and QC (open symbols) in the total number of collisions as functions of J at various T.

and $\nu_4 + \nu_5 - \nu_4$. The relative error of γ was estimated by the authors [24] at $\leq 5\,\%$.

Fig. 3, *a* presents the results of C3D calculations for the self-broadening of C_2H_2 absorption lines at various temperatures, while Fig. 3, *b* — shows the results of similar calculations for Q-lines of isotropic scattering. For comparison purposes, the vertical axis scale of the figures is the same. Fig. 4 shows the fractions of elastic collisions and collision complexes (also known as metastable dimers, Feshbach resonances, or quasibound complexes (QC)) in the total number of collisions at various J and T (for more on QC, see, e.g, [59]).

Comparison of Fig. 3, *a* and *b* shows that the contribution of elastic collisions to the self-broadening of C_2H_2 lines depends on J and T (recall that all types of collisions affect the broadening of IR absorption lines, whereas only inelastic collisions affect the broadening of Q-lines — isotropic Raman scattering). The increase of γ due to elastic collisions is particularly noticeable at low J and T. The fraction of elastic collisions increases with J reaching 60% at $J = 35$ (Fig. 4). It was also found that even at room temperature, a significant number of collision complexes form (Fig. 4); however, their contribution to broadening is substantial only at low temperatures. Interestingly, for $J = 0$ quasicomplexes reduce broadening, whereas for $J > 2$ they increase it (the nature of this effect remains unclear). The effect of QC on the broadening of scattering lines is somewhat less than for absorption lines, since only inelastic collisions are relevant in this case.

The results in Fig 3, *a, b* allow determination of the temperature dependence exponent n for line broadening. The traditional formula used is $\gamma(T) = \gamma(T_{\text{ref}}) \cdot (T_{\text{ref}}/\text{T})^n$, from which $n = \ln[\gamma(T)/\gamma(T_{\text{ref}})]/\ln(T_{\text{ref}}/T)$, where T_{ref} — some reference temperature. For these calculations, it was chosen as 298 K. Fig. 5, *a* presents the C3D calculation

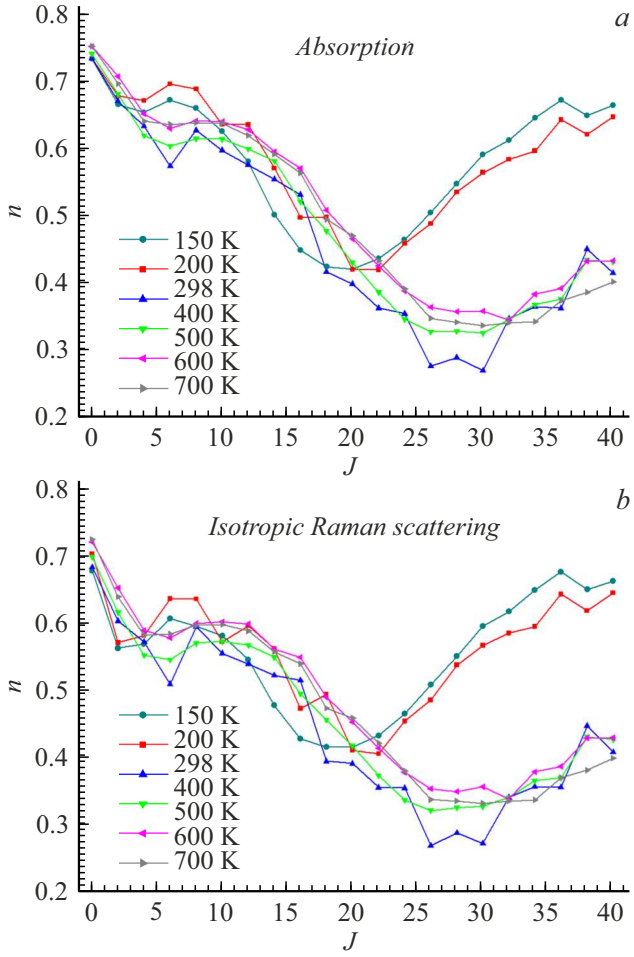

Figure 5. Temperature dependence exponent n of self-broadening for C_2H_2 absorption lines (a) and Q-lines of isotropic Raman scattering (b) for various J, calculated at different temperatures. $\gamma(T) = \gamma(T_{\text{ref}})(T_{\text{ref}}/T)^n$. $T_{\text{ref}} = 298$ K.

results for the n coefficient for absorption lines, and Fig. 5, *b* — for isotropic scattering.

Three important conclusions follow from Fig. 5: (1) the exponent n depends substantially on the rotational quantum number J, (2) the nature of the $n(J)$ dependence is nearly identical for absorption and scattering lines with only minor differences in numerical values, (3) the coefficient n depends significantly on temperature. An interesting effect is also observed: for $J > 20$ the $n(J)$ — dependence is an increasing function at $T < 200$ K, but a decreasing one at $T > 400$ K (except for high J). This effect, of course, requires further investigation. Conclusion (3) indicates the inadequacy of the traditionally used formula for $\gamma(T)$ dependence. Despite this, constant values n are frequently employed to describe temperature dependences of broadening. For example, in [26], the approximation formula for $\gamma_{\text{self}}(J, T)$ over a wide range J ($|m| \leq 34$) uses $n = 0.75$ for all $|m|$. Note that this convenient formula, derived by processing measurement results for several C_2H_2 bands, is valid only for temperatures close to room temperature.

Comparison of C3D-calculated $\gamma(T)$ and $n(T)$ dependences with experiment is shown in Fig. 6. Experimental data [42] were obtained by processing the measured spectrum of the $\nu_1+\nu_3$ $P(11)$ C_2H_2 absorption line using a speed-dependent Voigt profile (SDV profile). Results in Fig. 6, *b* were derived from data in Fig. 6, *a*. Fig. 6 shows that the nature of the $\gamma(T)$ and $n(T)$ dependences is the same for C3D calculations and experiment. Differences exist only in numerical values.

It is of interest to determine, within the classical approach, the effect of the electric quadrupole moment value on acetylene line broadening, since different authors use widely varying values in theoretical modeling. Literature values for the quadrupole moment of C_2H_2 range from 3 to 8.4 DÅ [45,60]. In this work, as in [24], the value measured in [54] $Q = 5.42$ DÅwas used for self-broadening coefficient calculations. Other (larger) experimental and calculated values for the quadrupole moment of C_2H_2 are given in [61]: 6.15 [62], 6.53 [63], 7.35 DÅ [64]. Fig. 7 shows $\gamma(J)$ dependences calculated at various Q values.

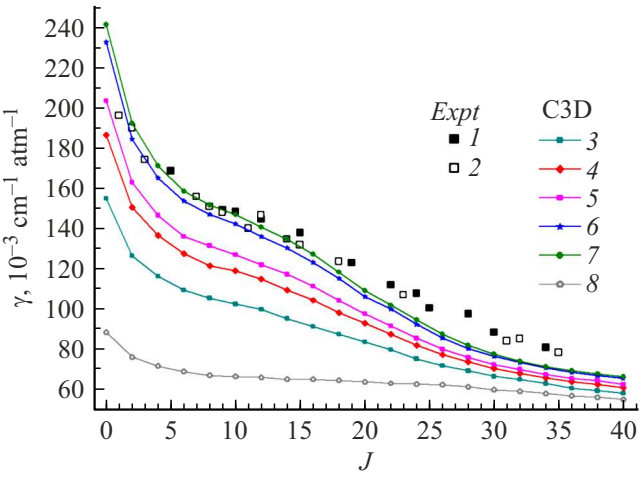

Figure 7. Effect of the quadrupole moment value of C_2H_2 on self-broadening of absorption lines. $T = 298$ K. Experiment: *1* — ν_5 *P*-branch [24], *2* — ν_5 *R*-branch [24]. C3D calculation: $Q = 3$ (*3*), 4.5 (*4*), 5.42 (*5*), 7.35 (*6*), 8.4 DÅ (*7*); $Q = 0$ (*8*).

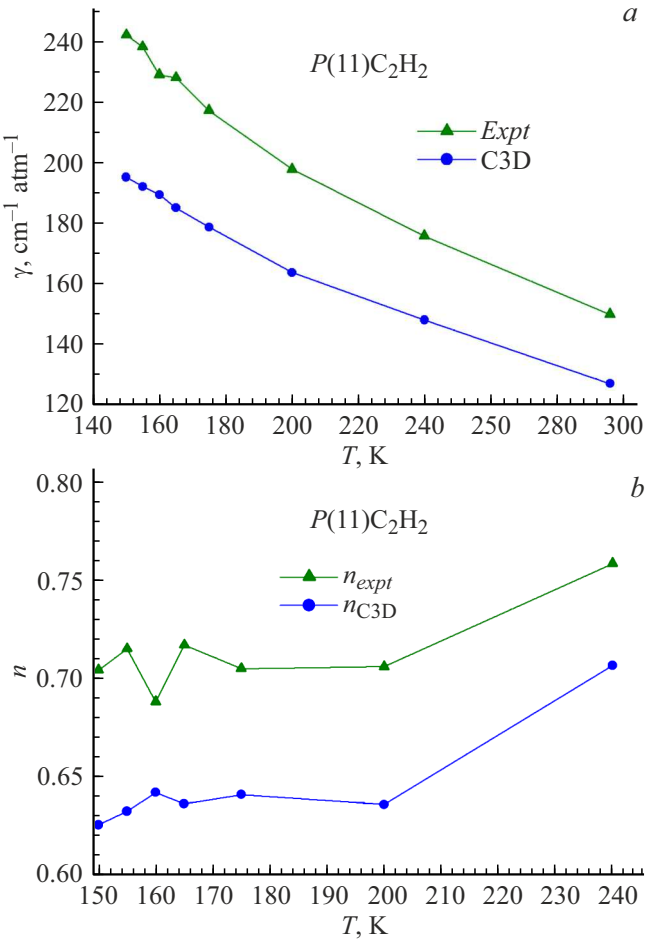

Figure 6. (*a*) Self-broadening coefficient $\gamma(T)$ of the absorption line $P(11)$ in the $\nu_1+\nu_3$ band of C_2H_2, experiment [42]; (*b*), temperature dependence of exponent $n(T)$ of self-broadening for the absorption line $P(11)$ in the $\nu_1+\nu_3$ band of C_2H_2. For experiment [42] $T_{ref} = 296$ K, for C3D calculations $T_{ref} = 298$ K. Experiment — triangles, calculations — circles.

The quadrupole moment value noticeably increases self-broadening, particularly at low and intermediate J. The contribution of the atom-atom part of the PES to broadening is small (Fig. 7 at $Q = 0$ — curve *8*). The quadrupole-quadrupole interaction plays the decisive role in shaping the J-dependence. A similar result was obtained in [24] using the semiclassical Robert-Bonamy method.

Quantitative differences between classical impact theory results and experiment are apparently related to imperfections in the intermolecular PES used in C3D calculations (both in the atom-atom and long-range parts). As evident from the above analysis, even such a seemingly simple quantity as the quadrupole moment remains insufficiently accurately known for C_2H_2 despite its strong influence on self-broadening. Concerning higher-order multipole moments (hexadecapole and above), their uncertainty is even greater.

6. Conclusion

Given the considerable number of theoretical works on self-broadening of C_2H_2 lines, the value of the results presented in this article may be questioned. In this regard, note the following. The vast majority of computational studies on impact broadening of molecular vibrational-rotational lines have been performed using semiclassical Anderson-Tsao-Curnutte (ATC) and/or Robert-Bonamy (RB) methods in their various (including recently modified) versions [7,22]. These methods rely on several simplifying approximations that distort the physics of collisional broadening (as noted, e.g., in [17–22,48,52,57]). However, these shortcomings are readily compensated by selecting appropriate fitting parameters for PES of more or less acceptable form to match specific measurement results, which is done in most theoretical works. Clearly, within such an approach, the

physics of the broadening process remains „behind the scenes“, and the predictive power of calculations for other conditions is questionable. Moreover, scatter in various experimental data can be significant (for self-broadening of C_2H_2 see, e.g., [24]). Therefore, correct modeling of impact broadening is possible only within a self-consistent approach (fully quantum or classical) using a reliable, maximally accurate PES. Unfortunately, self-consistency and accuracy of fully quantum methods are achieved at the cost of very time-consuming computations involving solution of large systems of coupled differential equations. Convergence issues also arise. Practical applications of the most accurate quantum CC/CS schemes remain limited even now to simple molecular systems at moderate temperatures. In this context, development of the classical method in collisional broadening theory is relevant. At the same time, the results obtained in this work should not be regarded as benchmark, but rather as a demonstration of the capabilities of the classical approach to the broadening problem and as „navigation“ for future theoretical and experimental studies under various conditions. Note also that further improvement of quantum chemical methods for obtaining maximally accurate ab initio PES is necessary to eliminate uncertainties in interpreting experimental data.

Acknowledgments

The author thanks O.G. Buzykin for assistance with numerical calculations.

Funding

The work was carried out as part of the state assignment of the NRC „Kurchatov Institute“.

Conflict of interest

The author declares that he has no conflict of interest.

Appendix

The exact 3D classical equations of motion for the system of two rigid linear molecules BC–AD (A, B, C, D — terminal atoms) in molecule-fixed coordinates have the following form:

$$\dot{R} = \frac{p_R}{\mu_{\mathrm{AD,BC}}}, \tag{A1}$$

$$\dot{\varphi} = \frac{(p_\varphi - J_y)}{\mu_{\mathrm{AD,BC}} R^2}, \tag{A2}$$

$$\dot{p}_R = \frac{(A+p_\theta)^2}{\mu_{\mathrm{AD,BC}} R^3 \sin^2\varphi} + \frac{(J_y - p_\varphi)^2}{\mu_{\mathrm{AD,BC}} R^3} - \frac{\partial V}{\partial R}, \tag{A3}$$

$$\dot{x}_1 = \frac{p_{x1}}{\mu_{\mathrm{BC}}} + \frac{y_1 \cos\varphi (A+p_\theta)}{\mu_{\mathrm{AD,BC}} R^2 \sin^2\varphi} + \frac{z_1 (J_y - p_\varphi)}{\mu_{\mathrm{AD,BC}} R^2}, \tag{A4}$$

$$\dot{y}_1 = \frac{p_{y1}}{\mu_{\mathrm{BC}}} - \frac{(x_1 \cos\varphi + z_1 \sin\varphi)(A+p_\theta)}{\mu_{\mathrm{AD,BC}} R^2 \sin^2\varphi}, \tag{A5}$$

$$\dot{z}_1 = \frac{p_{z1}}{\mu_{\mathrm{BC}}} + \frac{y_1 \sin\varphi (A+p_\theta)}{\mu_{\mathrm{AD,BC}} R^2 \sin^2\varphi} - \frac{x_1 (J_y - p_\varphi)}{\mu_{\mathrm{AD,BC}} R^2}, \tag{A6}$$

$$\dot{p}_{x1} = \frac{p_{y1} \cos\varphi (A+p_\theta)}{\mu_{\mathrm{AD,BC}} R^2 \sin^2\varphi} + \frac{p_{z1} (J_y - p_\varphi)}{\mu_{\mathrm{AD,BC}} R^2} - \frac{\partial V}{\partial x_1}, \tag{A7}$$

$$\dot{p}_{y1} = -\frac{(p_{x1} \cos\varphi + p_{z1} \sin\varphi)(A+p_\theta)}{\mu_{\mathrm{AD,BC}} R^2 \sin^2\varphi} - \frac{\partial V}{\partial y_1}, \tag{A8}$$

$$\dot{p}_{z1} = \frac{p_{y1} \sin\varphi (A+p_\theta)}{\mu_{\mathrm{AD,BC}} R^2 \sin^2\varphi} - \frac{p_{x1} (J_y - p_\varphi)}{\mu_{\mathrm{AD,BC}} R^2} - \frac{\partial V}{\partial z_1}, \tag{A9}$$

$$\dot{\theta} = \frac{(p_\theta + A)}{\mu_{\mathrm{AD,BC}} R^2 \sin^2\varphi}, \tag{A10}$$

$$\dot{p}_\varphi = \frac{\cos\varphi (A+p_\theta)^2}{\mu_{\mathrm{AD,BC}} R^2 \sin^3\varphi} - \frac{B(A+p_\theta)}{\mu_{\mathrm{AD,BC}} R^2 \sin^2\varphi}, \tag{A11}$$

$$\dot{x}_2 = \frac{p_{x2}}{\mu_{\mathrm{AD}}} + \frac{y_2 \cos\varphi (A+p_\theta)}{\mu_{\mathrm{AD,BC}} R^2 \sin^2\varphi} + \frac{z_2 (J_y - p_\varphi)}{\mu_{\mathrm{AD,BC}} R^2}, \tag{A12}$$

$$\dot{y}_2 = \frac{p_{y2}}{\mu_{\mathrm{AD}}} - \frac{(x_2 \cos\varphi + z_2 \sin\varphi)(A+p_\theta)}{\mu_{\mathrm{AD,BC}} R^2 \sin^2\varphi}, \tag{A13}$$

$$\dot{z}_2 = \frac{p_{z2}}{\mu_{\mathrm{AD}}} + \frac{y_2 \sin\varphi (A+p_\theta)}{\mu_{\mathrm{AD,BC}} R^2 \sin^2\varphi} - \frac{x_2 (J_y - p_\varphi)}{\mu_{\mathrm{AD,BC}} R^2}, \tag{A14}$$

$$\dot{p}_{x2} = \frac{p_{y2} \cos\varphi (A+p_\theta)}{\mu_{\mathrm{AD,BC}} R^2 \sin^2\varphi} + \frac{p_{z2} (J_y - p_\varphi)}{\mu_{\mathrm{AD,BC}} R^2} - \frac{\partial V}{\partial x_2}, \tag{A15}$$

$$\dot{p}_{y2} = \frac{(p_{x2} \cos\varphi + p_{z2} \sin\varphi)(A+p_\theta)}{\mu_{\mathrm{AD,BC}} R^2 \sin^2\varphi} - \frac{\partial V}{\partial y_2}, \tag{A16}$$

$$\dot{p}_{z2} = \frac{p_{y2} \sin\varphi (A+p_\theta)}{\mu_{\mathrm{AD,BC}} R^2 \sin^2\varphi} - \frac{p_{x2} (J_y - p_\varphi)}{\mu_{\mathrm{AD,BC}} R^2} - \frac{\partial V}{\partial z_2}, \tag{A17}$$

$\mu_{\mathrm{AD,BC}}$ — reduced mass of the AD–BC system; μ_{AD}, μ_{BC} — reduced masses of molecules AD and BC; $V = V(\mathbf{R}, \mathbf{r}_1, \mathbf{r}_2)$ — interaction potential between molecules AD and BC. $\dot{p}_\theta = 0$, $p_\theta = \mu_{\mathrm{AD,BC}} R^2 \dot{\theta} \sin^2\varphi - A = \mathrm{const}$ for the specific collision under consideration (determined by initial conditions).

$$\mathbf{J} = \mathbf{r} \times \mathbf{p},$$

$$J_{x1} = y_1 p_{z1} - z_1 p_{y1},\ J_{y1} = z_1 p_{x1} - x_1 p_{z1},$$

$$J_{z1} = x_1 p_{y1} - y_1 p_{z1},$$

$$J_{x2} = y_2 p_{z2} - z_2 p_{y2},\ J_{y2} = z_2 p_{x2} - x_2 p_{z2},$$

$$J_{z2} = x_2 p_{y2} - y_2 p_{z2},$$

$$A_1 = J_{x1} \sin\varphi - J_{z1} \cos\varphi,\ B_1 = J_{x1} \cos\varphi + J_{z1} \sin\varphi,$$

$$A_2 = J_{x2} \sin\varphi - J_{z2} \cos\varphi,\ B_2 = J_{x2} \cos\varphi + J_{z2} \sin\varphi,$$

$$J_y = J_{y1} + J_{y2},\ A = A_1 + A_2,\ B = B_1 + B_2.$$

References

[1] Herzberg G. *Molecular Spectra and Molecular Structure. II. Infrared and Raman Spectra of Polyatomic Molecules* (Van Nostrand, Princeton, 1945).

[2] K. Noll, R. Knacke, A. Tokunaga, J. Lacy, S. Beck, E. Serabyn. Icarus, **65** (2–3), 257–263 (1986). DOI: 10.1016/0019-1035(86)90138-7

[3] A. Coustenis, Th. Encrenaz, B. Bezard, G. Bjoraker, G. Graner, M. Dang-Nhu, E. Arie. Icarus, **102**, 240–260 (1993). DOI: 10.1006/icar.1993.1047

[4] M. Metsälä, F.M. Schmidt, M. Skyttä, O. Vaittinen, L. Halonen. J. Breath Res., **4** (4), 046003, 1–8 (2010). DOI: 10.1088/1752-7155/4/4/046003

[5] M. Frenklach. Phys. Chem. Chem. Phys., **4** (11), 2028–2037 (2002). DOI: 10.1039/b110045a

[6] Z.R. Quine, K.L. McNesby. Appl. Opt., **48** (16), 3075–3083 (2009). DOI: 10.1364/ao.48.003075

[7] J. Buldyreva, N. Lavrentieva, V. Starikov. *Collisional line broadening and shifting of atmospheric gases: A practical guide for line shape modeling by current semiclassical approaches* (Imperial College Press, 2011).

[8] J.-P. Bouanich, D. Lambot, G. Blanquet, J. Walrand. J. Mol. Spectrosc., **140** (2), 195–213 (1990). DOI: 10.1016/0022-2852(90)90134-C

[9] A.S. Pine. JQSRT, **50** (2), 149–166 (1993). DOI: 10.1016/0022-4073(93)90114-W

[10] J.-P. Bouanich, G. Blanquet, J.-C. Populaire, J. Walrand. J. Mol. Spectrosc., **190** (1), 7–14 (1998). DOI: 10.1006/jmsp.1998.7559

[11] A. Babay, M. Ibrahimi, V. Lemaire, B. Lemoine, F. Rohart, J.-P. Bouanich. JQSRT, **59** (3–5), 195–202 (1998). DOI: 10.1016/S0022-4073(97)00122-2

[12] S.W. Arteaga, C.M. Bejger, J.L. Gerecke, J.L. Hardwick, Z.T. Martin, J. Mayo et al. J. Mol. Spectrosc., **243**, 253–266 (2007). DOI: 10.1016/j.jms.2007.04.007

[13] M. Dhyne, L. Fissiaux, J.C. Populaire, M. Lepére. JQSRT, **110**, 358–366 (2009). DOI: 10.1016/j.jqsrt.2008.12.009

[14] M. Dhyne, P. Joubert, J.-C. Populaire, M. Lepére. JQSRT, **111** (7–8), 973–989 (2010). DOI: 10.1016/j.jqsrt.2009.12.004

[15] H. Rozario, J. Garber, C. Povey, D. Hurtmans, J. Buldyreva, A. Predoi-Cross. Mol. Phys., **110** (21–22), 2645–2663 (2012). DOI: 10.1080/00268976.2012.720040

[16] C. Povey, M. Guillorel-Obregon, A. Predoi-Cross, S.V. Ivanov, O.G. Buzykin, F. Thibault. Can. J. Phys., **91**, 896–905 (2013). DOI: 10.1139/cjp-2013-0031

[17] J. Buldyreva, S.V. Ivanov, L. Nguyen. J. Raman Spectrosc., **36**, 148–152 (2005). DOI: 10.1002/jrs.1283

[18] S.V. Ivanov, L. Nguyen, J. Buldyreva. J. Mol. Spectrosc., **233**, 60–67 (2005). DOI: 10.1016/j.jms.2005.05.014

[19] L. Nguyen, S.V. Ivanov, O.G. Buzykin, J. Buldyreva. J. Mol. Spectrosc., **239**, 101–107 (2006). DOI: 10.1016/j.jms.2006.05.020

[20] S.V. Ivanov, O.G. Buzykin. JQSRT, **111**, 2341–2353 (2010). DOI: 10.1016/j.jqsrt.2010.04.031

[21] F. Thibault, S.V. Ivanov, O.G. Buzykin, L. Gomez, M. Dhyne, P. Joubert, M. Lepére. JQSRT, **112**, 1429–1437 (2011). DOI: 10.1016/j.jqsrt.2011.02.011

[22] F. Thibault, R.Z. Martínez, D. Bermejo, S.V. Ivanov, O.G. Buzykin, Q. Ma. JQSRT, **142**, 17–24 (2014). DOI: 10.1016/j.jqsrt.2014.03.009

[23] J. Buldyreva, L. Nguyen. Mol. Phys. **102**, 1523–1535 (2004). DOI: 10.1080/00268970410001725837

[24] D. Lambot, A. Olivier, G. Blanquet, J. Walrand, J.-P. Bouanich. JQSRT, **45** (3), 145–155 (1991). DOI: 10.1016/0022-4073(91)90004-A

[25] D. Lambot, J.C. Populaire, J. Walrand, G. Blanquet, J.P. Bouanich. J. Mol. Spectrosc., **165**, 1–11 (1994). DOI: 10.1006/jmsp.1994.1107

[26] D. Jacquemart, J.-Y. Mandin, V. Dana, L. Régalia-Jarlot, X. Thomas, P. Von der Heyden. JQSRT, **75** (4), 397–422 (2002). DOI: 10.1016/S0022-4073(02)00017-1

[27] M. Lepére, G. Blanquet, J. Walrand, J.-P. Bouanich, M. Herman, J. Van der Auwera. J. Mol. Spectrosc., **242** (1), 25–30 (2007). DOI: 10.1016/j.jms.2007.01.004

[28] Sajid Muhammad Bilal, Es-sebbar E-touhami, Farooq Aamir. JQSRT, **148**, 1–12 (2014). DOI: 10.1016/j.jqsrt.2014.06.014

[29] A.S. Pine, J.P. Looney. J. Chem. Phys., **93**, 6942–6953 (1990). DOI: 10.1063/1.459471

[30] F. Herregotds, D. Hurtmans, J. Van der Auwera, M. Herman. J. Chem. Phys., **111**, 7954–7960 (1999). DOI: 10.1063/1.480129

[31] H. Valipour, D. Zimmermann. J. Chem. Phys., **114** (8), 3535–3545 (2001). DOI: 10.1063/1.1333022

[32] A. Lucchesini, M. de Rosa, D. Pelliccia, C. Gabbanini, S. Gozzini. Appl. Phys. B, **63**, 277–282 (1996). DOI: 10.1007/BF01833797

[33] C. Yelleswarapu, A. Sharma. JQSRT, **69** (2), 151–158 (2001). DOI: 10.1016/S0022-4073(00)00073-X

[34] P. Varanasi, R.P. Bangaru. JQSRT, **15**, 267–273 (1975). DOI: 10.1016/0022-4073(75)90149-1

[35] J.S. Wong. J. Mol. Spectrosc., **82**, 449–451 (1980). DOI: 10.1016/0022-2852(80)90128-9

[36] C.P. McRaven, M.J. Cich, G.V. Lopez, T.J. Sears, D. Hurtmans, A.W. Mantz. J. Mol. Spectrosc., **266** (1), 43–51 (2011). DOI: 10.1016/j.jms.2011.02.016

[37] J.S. Li, G. Durry, J. Cousin, L. Joly, B. Parvitte, V. Zeninari. JQSRT, **111** (15), 2332–2340 (2010). DOI: 10.1016/j.jqsrt.2010.04.025

[38] A.I. Nadezhdinskii, Ya.Ya. Ponurovskii. Spectrochim. Acta A, **66**, 807–810 (2007). DOI: 10.1016/j.saa.2006.10.040

[39] K.K. Lehmann. J. Chem. Phys., **146**, 094309 (2017). DOI: 10.1063/1.4977726

[40] W.C. Swann, S.L. Gilbert. JOSA B, **17** (7), 1263–1270 (2000). DOI: 10.1364/JOSAB.17.001263

[41] E.C. Gross, K.A. Tsang, T.J. Sears. J. Chem. Phys., **154**, 054305-1–054305-9 (2021); DOI: 10.1063/5.0036602

[42] M.J. Cich, C.P. McRaven, G.V. Lopez, T.J. Sears, D. Hurtmans, A.W. Mantz. Appl. Phys. B, **109**, 373–384 (2012). DOI: 10.1007/s00340-011-4829-0

[43] S.J. Cassady, W.Y. Peng, R.K. Hanson. JQSRT, **221**, 172–182 (2018). DOI: 10.1016/j.jqsrt.2018.09.031

[44] R. Georges, D. van der Vorst, M. Herman, D. Hurtmans. J. Mol. Spectrosc, **185** (1), 187–188 (1997). DOI: 10.1006/jmsp.1997.7372

[45] C. Povey, A. Predoi-Cross, D.R. Hurtmans. J. Mol. Spectrosc., **268**, 177–188 (2011). DOI: 10.1016/j.jms.2011.04.020

[46] J.-P. Bouanich, A. Predoi-Cross. Mol. Phys., **109** (17–18), 2071–2081 (2011). DOI: 10.1080/00268976.2011.599342

[47] Ayan kumar Pal, Naveen Kumar, R.J. Kshirsagar. JQSRT, **300**, 108510 (2023). DOI: 10.1016/j.jqsrt.2023.108510

[48] S.V. Ivanov, O.G. Buzykin. Mol. Phys., **106**, 1291–1302 (2008). DOI: 10.1080/00268970802270034

[49] G. Goldstein. *Classical Mechanics* (GITTLE, M., 1957) (in Russian).

[50] R.G. Gordon. J. Chem. Phys., **44** (8), 3083–3089 (1966). DOI: 10.1063/1.1727183

[51] R.G. Gordon. J. Chem. Phys., **45** (5), 1649–1655 (1966). DOI: 10.1063/1.1727808
[52] S.V. Ivanov, O.G. Buzykin. JQSRT, **119**, 84–94 (2013). DOI: 10.1016/j.jqsrt.2012.12.021
[53] Dzh. Girshfel'der, Ch. Kertiss, R. Berd. *Molekulyarnaya teoriya gazov i zhidkostej* (Inostrannaya literatura, Moskva, 1961). (in Russian).
[54] I.R. Dagg., A. Anderson, W. Smith, M. Missio, C.G. Joslin, L.A.A. Read. Can. J. Phys., **66** (5), 453–459 (1988). DOI: 10.1139/p88-074
[55] R.E. Langer. Phys. Rev., **51**, 669–676 (1937). DOI: 10.1103/PhysRev.51.669
[56] S. Chapman, S. Green. J. Chem. Phys., **67** (5), 2317–2331 (1977). DOI: 10.1063/1.435067
[57] S.V. Ivanov, O.G. Buzykin. JQSRT, **185**, 48–57 (2016). DOI: 10.1016/j.jqsrt.2016.08.017
[58] C.W. Gear. *Numerical Initial Value Problems in Ordinary Differential Equations* (Englewood Cliffs, Prentice-Hall, N.J., 1971).
[59] S.V. Ivanov. JQSRT, **177**, 269–282 (2016). DOI: 10.1016/j.jqsrt.2016.01.034
[60] C.G. Gray, K.E. Gubbins. *Theory of Molecular Fluids* (Oxford University Press, New York, 1984).
[61] J.M. Junquera-Hernandez, J. Sanchez-Marin, D. Maynau. Chem. Phys. Lett., **359**, 343–348 (2002). DOI: 10.1016/S0009-2614(02)00722-4
[62] S. Coriani, C. Hättig, P. Jorgensen, A. Rizzo, K. Ruud. J. Chem. Phys., **109**, 7176–7184 (1998). DOI: 10.1063/1.477399
[63] A. Halkier, S. Coriani. Chem. Phys. Lett., **303**, 408–412 (1999). DOI: 10.1016/S0009-2614(99)00269-9
[64] R.D. Amos, J.H. Williams. Chem. Phys. Lett., **66** (3) 471–474 (1979). DOI: 10.1016/0009-614(79)80319-X

Translated by J.Savelyeva